Reduction of thin-film ceria on Pt(111) by supported Pd nanoparticles probed with resonant photoemission

J. Matharu, Gregory Cabailh, R. Lindsay, C.L. Pang, D.C. Grinter, T. Skála, G. Thornton

Reduction of thin-film ceria on Pt(111) by supported Pd nanoparticles probed with resonant photoemission

J. Matharu[1], G. Cabailh[1], R. Lindsay[2], C.L. Pang[1], D.C. Grinter[1], T. Skála[3], G. Thornton[1,*]

[1]London Centre for Nanotechnology and Chemistry Department, University College London, 20 Gordon Street, London, WC1H 0AJ, UK

[2]Corrosion and Protection Centre, School of Materials, The University of Manchester, Sackville Street, Manchester, M13 9PL, UK

[3]Sincrotrone Trieste, Strada Statale 14, km 163.5, 34149 Basovizza-Trieste, Italy

[*] Corresponding author : g.thornton@ucl.ac.uk

Abstract

Local defects present in CeO_{2-x} films result in a mixture of Ce^{3+} and Ce^{4+} oxidation states. Previous studies of the Ce 3*d* region with XPS have shown that depositing metal nanoparticles on ceria films causes further reduction, with an increase in Ce^{3+} concentration. Here, we compare the use of XPS and resonant photoemission spectroscopy (RESPES) to estimate the concentration of Ce^{3+} and Ce^{4+} in CeO_{2-x} films grown on Pt (111), and the variation of this concentration as a function of Pd deposition. Due to the nature of the electronic structure of CeO_{2-x}, resonant peaks are observed for the 4*d*-4*f* transitions when the photon energy matches the resonant energy; ($h\nu$=121.0 eV) for Ce^{3+} and ($h\nu$=124.5 eV) for Ce^{4+}. This results in two discrete resonant photoemission peaks in valence band spectra. The ratio of the difference of these peaks with off-resonance scans gives an indication of the relative contribution of Ce^{3+}. Results from RESPES indicate reduction of CeO_{2-x} on deposition of Pd, confirming earlier findings from XPS studies.

Keywords: Ceria, thin film, resonant photoemission, palladium, RESPES, XPS

1. Introduction

Cerium dioxide is an industrially important material with a wide range of applications. It is the principal component of the modern three-way catalytic converter used in automobile

exhausts, which converts exhaust gases to less harmful products [1]. This process makes use of the capacity of ceria to store and release oxygen, which is promoted by precious metals such as Rh, Pd and Pt [1]. However, despite extensive investigation, detailed mechanistic insight into the operation of this catalyst is lacking.

Most of the surface science type studies of this catalytic system have been conducted by depositing metals on ultrathin single crystalline films of ceria to allow the use of electron based techniques. Such films can be grown on a variety of metal single crystal substrates including Pt(111) and Cu(111) [2, 3]. Typically, these ceria films exhibit oxygen vacancies formed either during growth or due to oxygen loss during annealing. These point defects lead to the reduction of some cerium atoms to the Ce^{3+} oxidation state, resulting in non-stoichiometric films, CeO_{2-x}.

Various metals have been deposited onto these CeO_{2-x} films, including Rh, Pd, Sn, Au and Ga [2-8], to examine their impact. In all but one case [9], there is substantive evidence of further oxide reduction. Our own X-ray photoelectron spectroscopy (XPS) measurements of the Ce 3*d* core level following Pd deposition onto CeO_{2-x}/Pt(111) [2] are in accord with these studies, showing an increase in Ce^{3+} concentration in the presence of Pd. XPS of the Ce 3*d* region has been used extensively to study the degree of reduction of various cerium compounds [10, 11].

Resonant photoemission spectroscopy (RESPES) is an alternative technique with which to examine the occupation of Ce 4*f* states. In particular, the Ce 4*d*-4*f* photoabsorption region has been investigated and the resonance peaks at 121.0 eV and 124.5 eV, arising due to Ce^{3+} and Ce^{4+} contributions [3, 5, 8, 12, 13] have been used to determine the ratio of these species. The degree of oxidation and changes in composition can then be monitored by the ratio of the heights of these resonance peaks, DCe^{3+}/DCe^{4+}. The height, *D*, is measured as the difference between the intensity of the peak in an on-resonance scan and an off-resonance scan.

Here, we directly compare XPS of the Ce 3*d* region and RESPES of the Ce 4*d*-4*f* transition in the study of the effect of Pd on ultrathin CeO_{2-x} films grown on a Pt(111) substrate. STM is also used to investigate the morphology of the synthesised films.

2. Experimental

Photoemission experiments were conducted at the Materials Science Beamline, Elettra Synchrotron, Trieste, Italy. This is a soft X-ray beamline, providing a monochromatic light source in the photon energy range 40-800 eV. The experimental vacuum chamber is fitted with a Specs Phoibos hemispherical energy analyser (150 mm mean radius with 9 channels), a fast entry load-lock, LEED optics, an ion sputtering gun, Ce and Pd evaporators, a dual source Mg/Al $K\alpha$ X-ray gun, a mass spectrometer and a sample heating system. The base pressure was $1x10^{-10}$ mbar.

Synthesis of ceria thin films was carried out using the method reported by Schierbaum [14]. A Pt (111) crystal was cleaned by cycles of Ar^+ sputtering, annealing in O_2 at 900 K and in ultra-high vacuum (UHV) at 1100 K. The clean surface was characterised by a 1×1 hexagonal LEED pattern, and the absence of contaminant peaks (principally carbon and oxygen [15]) in XP spectra, within the detection limits of the technique.

Cerium was deposited onto the Pt (111) substrate held at room temperature, then annealed under UHV to 1000 K. This gives rise to a 2×2 hexagonal LEED pattern due to the formation of a Pt-Ce alloy [14]. The deposited cerium was then oxidised by further annealing in 5×10^{-7} mbar O_2 at 1000 K, resulting in a 1.37×1.37 (±0.05) hexagonal LEED pattern, consistent with a recent study [16]. Palladium was deposited onto the CeO_{2-x}/Pt(111) system by e-beam heating of a Pd wire under UHV conditions.

XPS spectra were recorded for the Ce 3*d*, Pt 4*d*, Pd 3*d* and O 1*s* regions using an Al $K\alpha$ source at each stage of the experiment. The thicknesses of CeO_{2-x} and Pd deposits were calculated using the relative areas of overlayer (Ce 3*d*, Pd 3*d*) and substrate (Pt 4*d*) peaks [17]. Thicknesses are expressed in units of monolayer equivalence, MLE. A monolayer is defined as the number of Pt atoms in the top layer of the substrate; a monolayer equivalent is the number of close packed adsorbate species that would uniformly saturate the top layer of the substrate. RESPES scans of the valence band (VB, E_b = 0 - 16 eV) were recorded at each stage of Pd deposition using photon energies 113-131 eV. Spectra were normalised to the

beam current, monitored from a gold mesh located in front of the experimental UHV chamber.

STM images presented here were recorded in the constant current mode, using a commercial room temperature AFM/STM (Omicron GmbH) housed in a UHV analysis chamber with a base pressure of 1×10^{-10} mbar, at University College London. STM tips were prepared by electrochemical etching of W wire (Advent) in 2M NaOH, followed by degassing at ~500 K in UHV and Ar sputtering.

3. Results and discussion

STM of the Pt(111)/CeO_{2-x} surface (figure 1) shows that at 0.6 MLE coverage, islands of ceria cover approximately 30% of the Pt(111) substrate, and are predominantly of height 6 Å (see blue and black line profiles). This corresponds to two trilayers of CeO_2(111) (with a trilayer height of 3.1 Å). The red line profile is of a ceria island that has a partially formed second trilayer, consistent with ref. 18. By comparing with STM images of clean Pt(111) (not shown), regions between the ceria islands appear to be bare Pt(111).

Three ceria films were investigated, with estimated thicknesses: (i) 0.5 ± 0.2 MLE, (ii) 0.7 ± 0.2 MLE and (iii) 0.8 ± 0.2 MLE. XPS of the Ce 3*d* region (870-930 eV) was used to estimate the composition of the ceria as a function of Pd deposition for comparison with our previous study [2]. Due to final state effects, XPS spectra of the Ce 3*d* region consists of five doublet peaks, with two corresponding to Ce^{3+} states and the remaining three to Ce^{4+} states [10]. Figure 2 shows the Ce 3*d* XPS spectra of the as-prepared 0.8 MLE CeO_{2-x} film, and the same film following Pd deposition. A Shirley background has been removed from each spectrum [19], and the best fits with 5 Voigt (Gaussian-Lorentzian convolution [20]) doublet functions are displayed, labelled using an established notation [10]. Peak-widths and spin-orbit splitting (18.5 eV) were constrained during fitting. The binding energies and peak widths used are summarised in table 1, and mimic those employed in [3]. The most significant changes are an increase in intensity of the *v*' and *u*' peaks occasioned by Pd

deposition. The Ce^{3+} concentration, expressed as the ion concentration ratio, $r(Ce^{3+}/Ce^{4+})$ was calculated using an established procedure [11, 21, 22]. The values of $r(Ce^{3+}/Ce^{4+})$ for our films show that they have a small degree of non-stoichiometry and are partially reduced prior to Pd deposition, such that the composition of the films is (i) $CeO_{1.92}$, (ii) $CeO_{1.93}$ and (iii) $CeO_{1.93}$. Depositing Pd in sequential stages shows an increase in the Ce^{3+} concentration (and thus an increase in $r(Ce^{3+}/Ce^{4+})$. These results are summarised in table 2.

RESPES spectra were recorded for films (ii) and (iii) before and after Pd deposition. Resonant photoemission peaks for Ce^{3+} and Ce^{4+} states appear at binding energies of 1.5 eV and 4 eV, respectively, at photon energies of 121.0 eV (Ce^{3+}) and 124.5 eV (Ce^{4+}). An examination of the ratio, DCe^{3+}/DCe^{4+} of the intensities of these two features gives an indication of the composition of the ceria films and the Ce^{3+} concentration. The intensities of the resonant peaks, DCe^{3+} and DCe^{4+} were measured as the difference between the on-resonance scans and an off-resonance scan (the scan measured at 115 eV). Figure 3 shows these scans for film (iii) before and after Pd deposition, with subtraction curves (on- minus off-resonance) also displayed. These scans were normalised to the mesh current and the backgrounds were aligned. The resonant peak Ce^{3+} increases slightly on Pd deposition and increases the ratio DCe^{3+}/DCe^{4+}. These results are summarised in table 2.

The three films studied here have a thickness range of 0.5-0.8 MLE. XPS peak fitting of Ce 3*d* spectra for the three films shows Ce^{3+}/Ce^{4+} ion concentration ratios in the range 0.134-0.187, with a negative correlation suggested by decreasing ratio with increasing film thickness. Previously we reported a CeO_{2-x} film consisting of three O-Ce-O layers grown on Pt(111) to have a Ce^{3+}/Ce^{4+} ratio of 0.125 ± 0.04 [2]. This lower value is likely due to the increased thickness in our earlier work, with the stability of defects such as oxygen vacancies stabilised at the interface between the oxide film and the metal [23, 24].

There is qualitative agreement between the XPS- and RESPES-derived Ce^{3+}/Ce^{4+} changes introduced by Pd deposition, as seen in Table 2. However, it is clear that quantitative agreement is lacking, with a difference in a factor of 1.6 in most of the values. The dominant cause of this discrepancy is expected to arise from the difference in surface sensitivities of the two methods, arising from the shorter photoelectron escape depth for

RESPES. This will serve to enhance any Pd-induced effect. These results are consistent with previous RESPES experiments of metals on ceria [3, 5-8, 13], although the effect of Pd on CeO_{2-x} is much weaker than for instance Ga [8]. This is in line with the charge transfer model of reduction predicted by theoretical calculations [2].

4. Summary

XPS and RESPES have been used to study the interaction between deposited Pd and thin-films of CeO_{2-x} on a Pt(111) substrate. The use of RESPES analysis of the valence band provides a higher degree of sensitivity to surface changes in the top O-Ce-O trilayer than XPS. In particular, the relative Ce^{3+} concentration of the film has been used as a measure of reduction and has been estimated by both analysis of Ce 3*d* XPS spectra and the ratio of resonant peaks in the valence band. XPS spectra have shown that for films of three different thicknesses, incremental Pd deposition results in an increase in the ion concentration ratio, $r(Ce^{3+}/Ce^{4+})$. RESPES shows that the resonant peak intensity ratio DCe^{3+}/DCe^{4+} increases upon Pd deposition, confirming earlier XPS measurements. In principle, reduction of the films could be due to oxygen vacancies created on deposition of Pd or charge transfer from the Pd nanoparticles to the ceria films. Earlier theoretical calculations point to the latter explanation [2].

Acknowledgements

The research leading to these results has received funding from the European Community Seventh Framework Programme (FP7/2007-2013) under grant agreement 226716, as well as COST action D41. The Materials Science Beamline is supported by the Ministry of Education of the Czech Republic under grant no. LA08022.

GT and RL devised the experiments, all authors took part in the experiment, JM, CG and DC analysed the data, and all authors contributed to writing the manuscript.

References

[1] A. Trovarelli, Catalysis by Ceria and Related Materials, Vol. 2, 2000, Imperial College Press, London.

[2] E.L. Wilson, R. Grau-Crespo, C.L. Pang, G. Cabailh, Q. Chen, J.A. Purton, C.R.A. Catlow, W.A. Brown, N.H. de Leeuw, G. Thornton, J. Phys. Chem. C, 112 (2008) 10918.

[3] T. Skála, F. Sutara, M. Skoda, K.C. Prince, V. Matolín, J. Phys. Condens. Matter, 21 (2009) 055005.

[4] A. Pfau, K.D. Schierbaum, W. Gopel, Surf. Sci, 331 (1995) 1479.

[5] V. Matolín, M. Cabala, V. Chab, I. Matolínova, K.C. Prince, M. Skoda, F. Sutara, T. Skála, K. Veltruská, Surf. Interface Anal., 40 (2008) 225.

[6] M. Skoda, M. Cabala, V. Cháb, K.C. Prince, L. Sedlacek, T. Skála, F. Sutara, V. Matolín, Appl. Surf. Sci., 254 (2008) 4375.

[7] M. Skoda, M. Cabala, I. Matolínova, K.C. Prince, T. Skála, F. Sutara, K. Veltruská, V. Matolín, J. Chem. Phys., 130 (2009) 034703.

[8] T. Skála, F. Sutara, M. Cabala, M. Skoda, K.C. Prince, V. Matolín, Appl. Surf. Sci., 254 (2008) 6860.

[9] S.D. Senanayake, J. Zhou, A.P. Baddorf, D.R. Mullins, Surf. Sci. 601 (2007) 3215.

[10] P. Burroughs, A. Hamnett, A.F. Orchard, G. Thornton, J. Chem. Soc. Dalton Trans., (1976) 1686.

[11] M. Romeo, K. Bak, J. El Fallah, F. Le Normand, L. Hilaire, Surf. Interf. Anal., 20 (1993) 508.

[12] M. Matsumoto, K. Soda, K. Ichikawa, S. Tanaka, Y. Taguchi, K. Jouda, O. Aita, Y. Tezuka, S. Shin, Phys. Rev. B: Condens. Matter, 50 (1994) 11340.

[13] V. Matolín, L. Sedlacek, I. Matolínova, F. Sutara, T. Skála, B. Smid, J. Libra, V. Nehasil, K.C. Prince, J. Phys. Chem. C, 112 (2008) 3751.

[14] K.D. Schierbaum, Surf. Sci., 399 (1998) 29.

[15] M. Grunze, H. Ruppender, O. Elshazly, J. Vac. Sci. Technol. A (1988) 1266.

[16] D.C. Grinter, R. Ithnin, C.L. Pang, G. Thornton, J. Phys. Chem. C, 114 (2010) 17036.

[17] D. Briggs, M.P. Seah (Eds.), Practical Surface Analysis by Auger and X-ray Photoelectron Spectroscopy, 1987, John Wiley & Sons

[18] U. Berner, K.D. Schierbaum, Phys. Rev. Lett., 65 (2002) 235404.

[19] D.A. Shirley, Phys. Rev. B, 5 (1972) 4709.

[20] E.E. Whiting, J. Quant. Spectrosc. Radiat. Transfer, 8 (1968) 1379.

[21] E. Preisler, O.J. Marsh, R.A. Beach, T.C. McGill, J. Vac. Sci. Tech. B, 19(4) (2001) 1611.

[22] F. Zhang, P. Wang, J. Koberstein, S. Khalid, S-W. Chan, Surf. Interf. Anal., 563 (2004) 74.

[23] S. Eck, C. Castellarin-Cudia, S. Surnev, M.G. Ramsey, F.P. Netzer, Surf. Sci., 520 (2002), 173.

[24] T.X.T. Sayle, S.C. Parker, C.R.A. Catlow, J. Phys. Chem. C, 98 (1994), 13625

	Binding energy/ eV	Branching ratio	Gaussian width/eV	Lorentzian width/eV
v_o, u_o	880.2 898.7	0.56	1.73	0.93
v, u	882.5 901.0	0.70	1.03	1.35
v', u'	884.8 903.3	0.56	0.57	4.47
v'', u''	888.9 907.4	0.61	2.09	4.01
v''', u'''	898.5 916.9	0.71	1.26	1.60

Table 1 : Binding energies, branching ratios, Lorentzian and Gaussian widths used in the fitting of Ce 3*d* XPS spectra.

Film	CeO_{2-x}	Pd thickness	XPS	RESPES

	film thickness MLE	MLE	$r(Ce3+/Ce4+)$	$DCe3+/DCe4+$
(i)	0.5 ± 0.2	0	0.155 ± 0.01	
		0.4 ± 0.3	0.174 ± 0.01	
		1.3 ± 0.9	0.187 ± 0.02	
(ii)	0.7 ± 0.2	0	0.140 ± 0.01	0.220 ± 0.01
		0.3 ± 0.2	0.151 ± 0.01	0.244 ± 0.01
		0.7 ± 0.6	0.156 ± 0.02	0.255 ± 0.01
(iii)	0.8 ± 0.2	0	0.134 ± 0.01	0.212 ± 0.01
		0.9 ± 0.3	0.161 ± 0.02	0.320 ± 0.01

Table 2 : Ion concentration, $r(Ce^{3+}/Ce^{4+})$ and resonant peak intensity ratio, DCe^{3+}/DCe^{4+} for films (i), (ii) and (iii) before and after successive Pd deposition. The error bars on the ratios are derived solely from the fitting procedure.

FIGURE CAPTIONS

Figure 1: An STM image (150×150 nm^2, V_s = +1.76 V, I_t = 0.50 nA) and associated line profiles of a typical CeO_{2-x}(111) ultrathin film of coverage ~0.6 MLE, which produced a 1.37×1.37 LEED pattern as shown inset (Beam energy = 70 eV). Line profiles are shown of islands ~6 Å thick.

Figure 2: Top: Ce 3*d* Al Kα XPS spectrum of (a) the as-prepared 0.8 MLE CeO_{2-x} film, and (b) the same film following 0.9 MLE Pd deposition. Blue and red curves correspond to Ce^{3+} and Ce^{4+} Voigt contributions, respectively; the green curves are the sum of these calculated doublets. Spectra are normalised to the same maximum intensity for comparison. Bottom: comparison of the fitted components.

Figure 3: Top: Valence band scans for (a) the as-prepared 0.8 MLE CeO_{2-x} film, and (b) the same following 0.9 MLE Pd deposition. In each case three scans are displayed measured at different photon energies. The black curves correspond to off-resonance scans ($h\nu$=115 eV), the blue and red to on-resonance scans for Ce^{3+} ($h\nu$=121.0 eV) and Ce^{4+} ($h\nu$=124.5 eV), respectively. Spectra are normalised to the mesh current and scaled to the same maximum intensity. Bottom: Difference spectra (on- minus off-resonance) for the 0.8 MLE CeO_{2-x} film before and after Pd deposition, derived from the spectra in (a). For the as-prepared film, the difference spectra measured with an on-resonance photon energy of $h\nu$=121.0 eV ($h\nu$=124.5 eV) are displayed in blue (red). For the film after deposition of 0.9 MLE, the corresponding difference spectra are shown in orange and lilac.

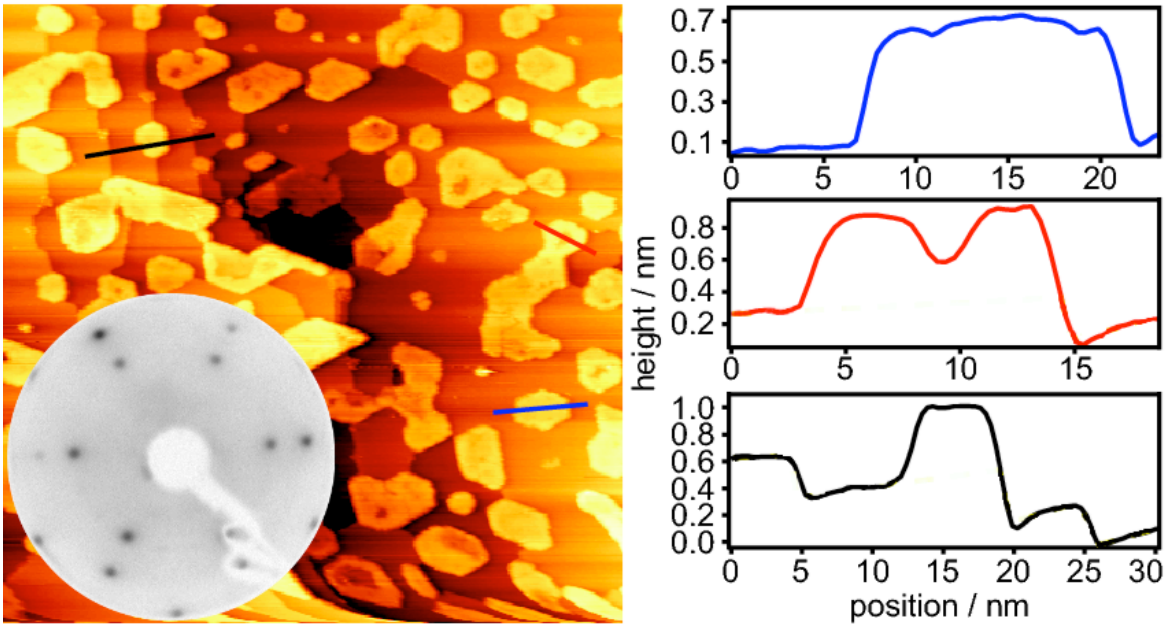

Figure 1

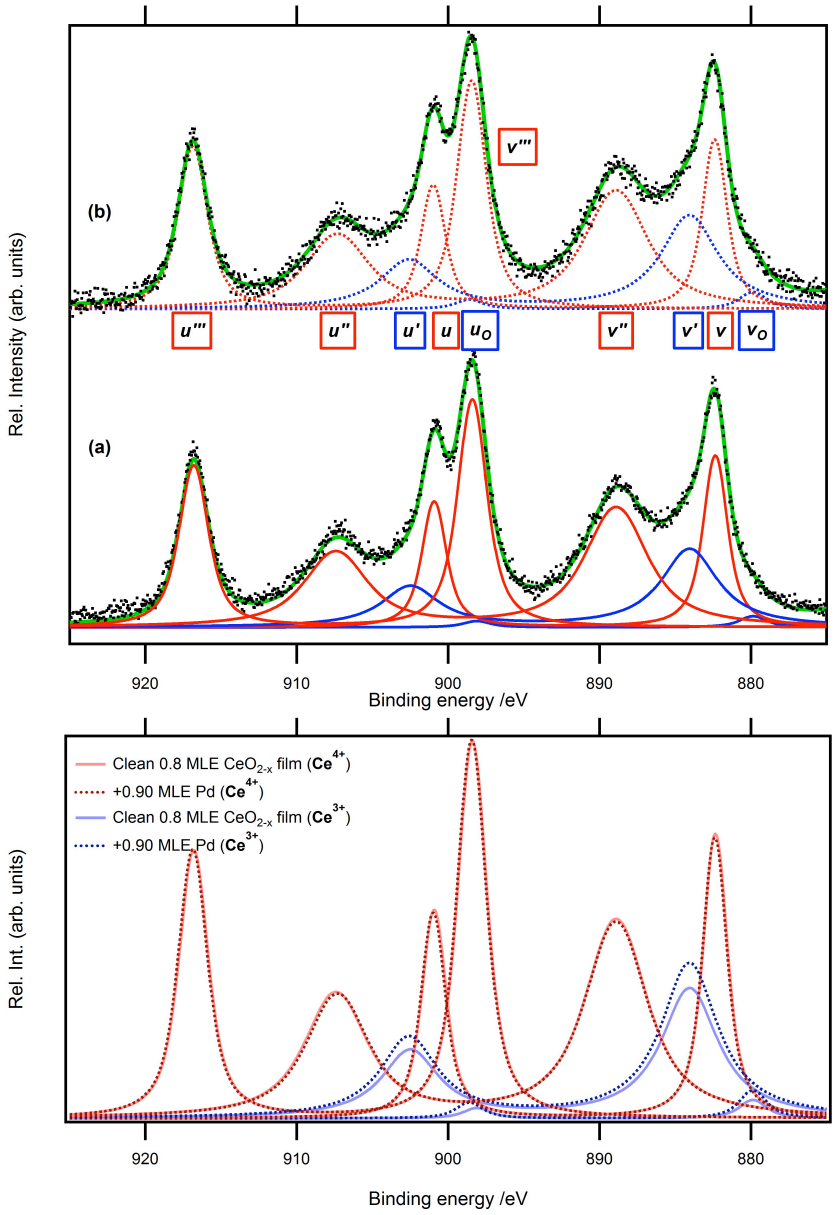
(b)
(a)
v'''
u'''
u''
u'
u
u_O
v''
v'
v
v_O
Rel. Intensity (arb. units)
920
910
900
890
880
Binding energy /eV
Clean 0.8 MLE CeO2-x film (Ce4+)
+0.90 MLE Pd (Ce4+)
Clean 0.8 MLE CeO2-x film (Ce3+)
+0.90 MLE Pd (Ce3+)
Rel. Int. (arb. units)
920
910
900
890
880
Binding energy /eV

Figure 2

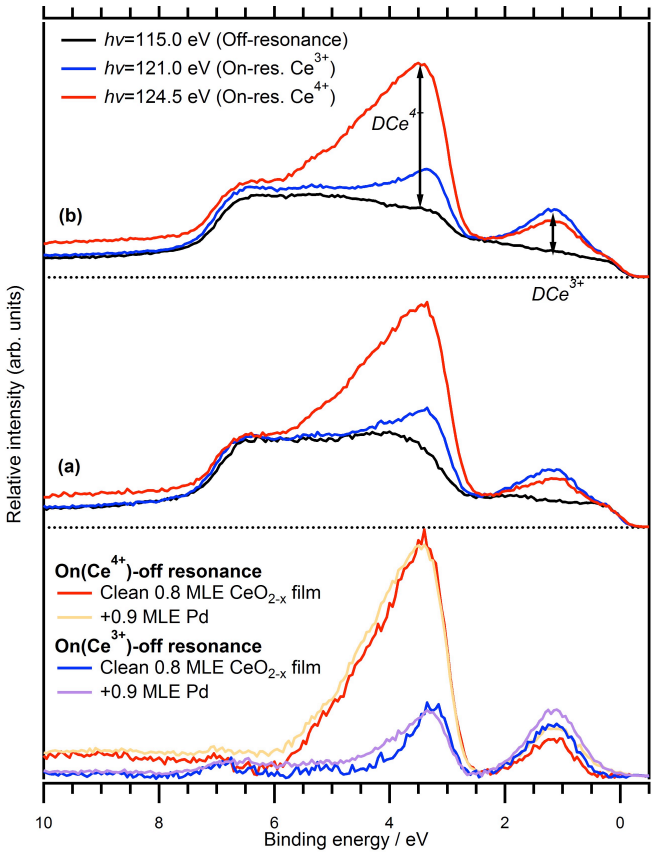
hv=115.0 eV (Off-resonance)
hv=121.0 eV (On-res. Ce3+)
hv=124.5 eV (On-res. Ce4+)
DCe4+
(b)
DCe3+
(a)
Relative intensity (arb. units)
On(Ce4+)-off resonance
Clean 0.8 MLE CeO2-x film
+0.9 MLE Pd
On(Ce3+)-off resonance
Clean 0.8 MLE CeO2-x film
+0.9 MLE Pd
10
8
6
4
2
0
Binding energy / eV

Figure 3